2018 IEEE Conference on Control Technology and Applications (CCTA)
Copenhagen, Denmark, August 21-24, 2018

Multi-rotor wind turbine control challenge - A benchmark for advanced control development

Kim Hylling Sørensen[2], Torben Knudsen[1], Oliver Tierdad Filsoof[2],
Tobias Gybel Hovgaard[2], Jacob Deleuran Grunnet[2], Julio Xavier Vianna Neto[2] and Rafal Wisniewski[1]

***Abstract*— We consider the control of a multi-rotor wind turbine consisting of two or more nacelles, each with at least a rotor and a generator, fixed to the same load carrying structure. We present a set of control challenges and provide an easily accessible simulation model as a benchmark for development of new ideas and comparison of methods for multi-rotor control. The control objective for the multi-rotor is to minimize the fatigue in the structure supporting the nacelles, while maximizing generated power and observing constraints on, e.g., rotational speed, rotor thrust, etc. We describe a model including the basic dynamics for a four rotor turbine. For this model an open Simulink model is made available for download. Furthermore, we provide an animation tool for visualization of the movement of the support structure during simulations. As an example we design and test a controller using the simulator. The is test completed for normal turbulence conditions obtaining significant fatigue load reductions with a limited power loss.**

I. INTRODUCTION

At the start of the millennium, an ever increasing (in fact mathematically exponential) growth in turbine size with time had been documented by manufacturers and was a general industry trend [1]. Even though this growth rate has leveled somewhat, rated power is now exceeding 4 MW for onshore turbines and 9 MW for offshore. The interest in yet larger wind turbines, especially for offshore markets, is reflected in the UPWIND project. This major project of the EU 6 Framework Program addresses a wide range of wind energy issues, including up-scaling, by evaluating the technical and economic issues in developing wind turbines of 10 to 20 MW capacity [2]. All commercially successful wind turbines have been horizontal axis single rotor turbines (SRT) with one rotor and nacelle placed on top of a tower. The future challenges in extending the conventional SRT concept to achieve higher ratings are considerable. The weight increases by the cube of the rotor radius while the power increases with the square - this means that material cost increases faster than power gained. An alternative to SRT is a multi-rotor turbine (MRT) i.e. one with more rotors on the same support structure (tower). MRTs have been known back in the history from at least 1873 and more recent versions have appeared from Lagerwey Wind [3] and from Vestas Wind Systems.

[1]Torben Knudsen and Rafal Wisniewski are with Department of Electronic Systems Section of Automation and Control at Aalborg University Denmark {tk,raf}@es.aau.dk

[2]Kim Hylling Sørensen, Oliver Tierdad Filsoof, Tobias Gybel Hovgaard, Jacob Deleuran Grunnet and Julio Xavier Vianna Neto are with Vestas Wind Systems Denmark
{kihso,olfil,togho,jadgr, and juxav}@vestas.com

If we take a MRT with n rotors which have the same total rated power as a SRT then the weight of the n rotors will be $\frac{1}{\sqrt{n}}$ times the weight of the single rotor according to the cube-square law [4].

The advantages of MRT over SRT are: [3], [4]:

- Lower total weight as well as rotor weight for the same power rating.
- Higher energy production as rotors can operate individually at e.g. different rotational speed in wind shear.
- Reduced transport and installation cost as well as easier access to remote areas due to smaller turbine parts.

One of the disadvantages is the increased structural complexity and thus the risk of increasing fatigue loads due to oscillations as the structural modes are excited more by having multiple nacelles and rotors attached to it. In the scarce literature, [3], [4], [5], [6] no investigation of this fatigue load challenge has been found.

Many types of advanced control methods have been applied to minimize fatigue loads on SRTs. Among these are Linear Quadratic Gaussian [7], [8], [9], Stochastic Disturbance Accommodating controller [10], [11], [12] and Model Predictive Control [13], [14], [15] but there is no reports on the control of MRT in the literature. Thus, the controllers addressing this challenge will be the first state-of-the-art on control of MRT.

This paper presents an MRT configuration with four 5 MW nacelles and rotors attached to a supporting structure as illustrated in Fig. 1. This four-rotor turbine (4-RT) structure is similar to the existing Vestas multi-rotor demonstrator seen in Fig. 2. For the simulation model, we use four of the 5 MW NREL reference wind turbines [16], giving a total rated power of 20 MW. Each NREL turbine can be operated with its own independent control system, like it would in an SRT configuration [17]. The rotors are spaced vertically

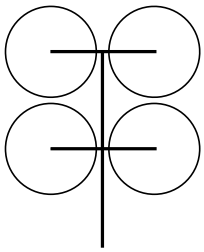

Fig. 1: Four rotor turbine (4-RT) - Down-wind view

and horizontally with 10 % of the rotor diameter. All rotors rotates in the same clock wise (CW) direction. The main

parameters and naming convention for the rotors can be seen in Tab. I.

TABLE I: (a) Main parameters for the NREL 4-RT. (b) Front view illustration of the NREL 4-RT.

(a)

Rotors	4
Rotor rated power	5 MW
Rated wind speed	12.4 m/s
Rotor diameter	126.0 m
Rotor Spacing	12.6 m
Hub height low	90.0 m
Hub height high	228.6 m
Upper level tip height	291.6 m

(b)

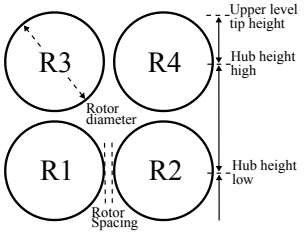

A. Challenge Description and Criteria's

The benchmark controller (BMC) consist of four individual NREL controllers, each controlling one rotor, on the entire 4-RT structure. The challenge is to design a new baseline controller (BLC) that reduces the movements of the structure while maintaining power and not overusing the pitch actuators.

In order to compare the BLC performance with the BMC it is important to compare for varying environmental parameters such as wind speeds and turbulence intensities (TI). Three ambient weather scenarios have been selected and are seen in Tab. II. Normal turbulence is the weather which the turbine experiences most of its lifetime. Extreme turbulence is a rare weather event occurring on a 50-year cycle. Power Curve (PC) is an artificial defined weather condition for evaluating power curves. Normal and extreme turbulence models (NTM and ETM) are used for this. The models require a cut-in and cut-out wind speed, V_{in} and V_{out} and a TI-90% quantile value as inputs. To get more insight in these models and weather conditions see IEC 61400-1 [18].

TABLE II: Benchmark weather conditions

Weather Conditions	**Wind Speed:**V_{in}-V_{out}	**TI-90% Quantile**
Normal Turbulence	2-20 m/s in steps of 2	0.15
Exstreme Turbulence	2-20 m/s in steps of 2	0.35
Power Curve	2-20 m/s in steps of 1	0.10 (flat)

For the weather conditions a set of performance indicators must be evaluated against the performance of the BMC. This set of parameters are tabulated in Tab. III. The first 7 parameters are the damage equivalent loads (DELs). The DELs are evaluated with normal and extreme turbulence conditions because it is here the structure experiences most dominating and critical loads.

The power production is important to compare, because it is possible to make a good BLC which dampens all structural movements but sacrifices power production too much. The BLC must at maximum loose 3 % of the produced power compared to the BMC. The last parameter is the accumulated pitch distance traveled (Acc. PDT) which indicates if pitch actuators are being overused. An 10 % increase in Acc. PDT is acceptable to achieve the control objectives.

TABLE III: Benchmark Parameters, evaluation methods, and success criteria:

Parameter Evaluation	**Method**	**Success Criteria**
DEL: Tower Root Moment (Mx)	NTM, ETM	BLC $\leqq$ BMC
DEL: Yaw 1 Moment Mz	NTM, ETM	BLC $\leqq$ BMC
DEL: Yaw 2 Moment Mz	NTM, ETM	BLC $\leqq$ BMC
DEL: Arm 1 Root Moment Mx	NTM, ETM	BLC $\leqq$ BMC
DEL: Arm 2 Root Moment Mx	NTM, ETM	BLC $\leqq$ BMC
DEL: Arm 3 Root Moment Mx	NTM, ETM	BLC $\leqq$ BMC
DEL: Arm 4 Root Moment Mx	NTM, ETM	BLC $\leqq$ BMC
Mean: Power Production	NTM, PC	BLC $\geqq$ BMC-3%
Sum: Pitch Distance Traveled	Only NTM	BLC $\leqq$ BMC+10%

The tower root moment, yaw moments and arm torsions are chosen as evaluation parameters for the DELs. These are important for the MRT because they represent design critical mechanical properties. If design limits are exceed this will be fatal for the turbine.

In the following sections a description of the support structure and the development of the dynamic model are presented along with a description of the simulation model which is made available to researchers for development of new controllers. Following this, the control problem is discussed and an example control solution is developed. The performance of the controller is evaluated compared to the benchmark.

Fig. 2: Existing Vestas MRT demonstrator consisting of 4 V29 225kW nacelles and rotors. The demonstrator is situated at Risø DTU in Roskilde Denmark.

II. STRUCTURAL MODEL

In this section, a state-space model of an MRT with four three-bladed rotors is presented. This includes a description of the degrees of freedom (DOFs), derivation of the dynamic

equations of motion using Lagrange equations as well as the state-space representation of the model.

The following model assumptions are taken:

- No gravitational loads are included due to limited effect on frequency response
- No aerodynamic stiffening and damping from rotors
- Only trust forces are applied
- Blades are not included in the model
- No arm bending dynamics i.e. very stiff arms

A. Degrees of Freedom and Geometry

To describe the structural dynamics of the 4-RT, 10 DOFs are chosen. The first 4 DOFs represent the two tower sections' fore-aft bending. This includes 2 rotational components, $\theta_{xP0}(t)$ and $\theta_{xP1}(t)$ and 2 translation components, $u_{yP0}(t)$ and $u_{yP1}(t)$. Subscript P0 refers to the lower platform and P1 to the upper platform. It is important to maintain a balanced thrust force across the rotors on each platform to prevent large torsional moments on the tower. Therefore two rotational DOFs are used to represent tower torsion of each section, $\theta_{zP0}(t)$ and $\theta_{zP1}(t)$. Furthermore, each arm tip have a rotational DOF to represent arm torsion, $\theta_{xR1}(t)$, $\theta_{xR2}(t)$, $\theta_{xR3}(t)$ and $\theta_{xR4}(t)$. Subscript $R1$ and $R2$ refers to each nacelle and the adjacent arm structure on $P0$, and likewise for subscripts $R3$ and $R4$ on $P1$. Arm torsion is important to consider as the rotor thrust force acting on a point which is offset relative to the center of the support arm is prone to induce torsional movements as seen from L_{zN} in Fig. 3.

The stiffnesses and masses for the two tower sections are calculated using classical-beam theory. The structural natural frequencies and a description of those are listed in Tab. IV.

TABLE IV: Mode shapes and frequencies for the 4-RT.

Mode	Description	Freq. [Hz]
1	First tower fore-aft	0.12
2	Symmetric yaw	0.13
3	Second tower fore-aft	0.40
4	Asymmetric yaw	0.57
5	Second tower fore-aft coupled with arm torsion	0.98
6	Symmetric arm torsion of upper platform	2.29
7	Symmetric arm torsion of lower platform	2.85
8	Asymmetric arm torsion of upper platform	3.14
9	Asymmetric arm torsion of lower platform	3.16
10	Arm torsion coupled with rotational tower	7.21

The dimensions of the structure and locations of the point masses are shown in Fig. 3 and listed in Tab. V.

B. Equations of Motion and State-Space Representation

The equations of motion are derived using Lagrange equation

$$\frac{d}{dt}\left(\frac{\partial T}{\partial \dot{q}_j}\right) - \frac{\partial T}{\partial q_j} + \frac{\partial V}{\partial q_j} = Q_j^{(n)}, \qquad j = 1, 2, ..., n \quad (1)$$

where T is the kinetic energy, V is the potential energy, q_j is the generalized coordinates of the system where n is the number of generalized coordinates and $Q_j^{(n)}$ is the non-conservative generalized force.

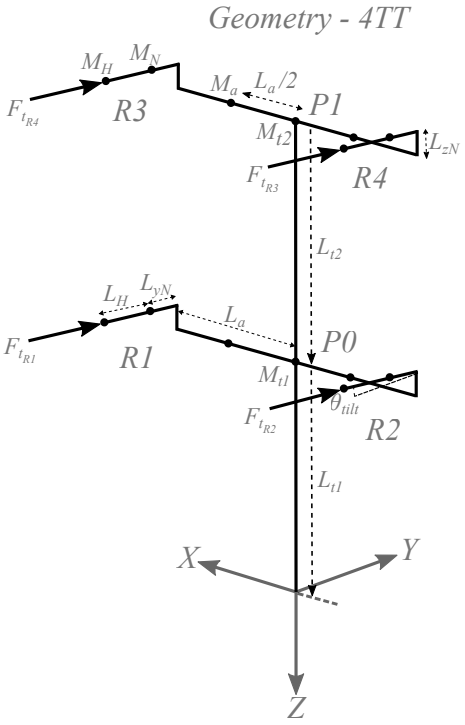

Fig. 3: Dimensions and location of masses on the MRT structure.

TABLE V: Material properties for the geometry shown in Fig. 3.

Parameter		Value	
L_a	Arm length	66.15	[m]
L_{zN}	Nacelle offset	1	[m]
L_{yN}	Length to nacelle CG	1.96256	[mm]
L_H	Length to hub	5.01910	[m]
L_{t1}	First tower section height	90	[m]
L_{t2}	Second tower section height	138.6	[m]
θ_{tilt}	Nacelle tilt angle	5	[deg]
M_H	Hub mass including blade mass	109930	[kg]
M_N	Nacelle mass	215000	[kg]
M_a	Arm mass	129029	[kg]
M_{t1}	First tower section mass	901690	[kg]
M_{t2}	Second tower section mass	567065	[kg]

T is calculated according to:

$$T = \frac{1}{2}\int_{V_v} \rho \{\dot{r}\}^T \{\dot{r}\}\, dV_v \quad (2)$$

where r is the position vector of the body, ρ is the density of the body and V_v is the volume of the body.

The non-conservative generalized force can be calculated as:

$$Q_j^{(n)} = \sum_k \left(F_{xk}\frac{\partial x_k}{\partial q_j} + F_{yk}\frac{\partial y_k}{\partial q_j} + F_{zk}\frac{\partial z_k}{\partial q_j} \right) \quad (3)$$

where F_{xk}, F_{yk} and F_{zk} represent external forces acting on the system. In our case, the external forces come from the trust forces from the rotors, see Fig. 3. k is the number of

forces acting on the system. By inserting expressions for T, V and $Q_j^{(n)}$ into (1) and performing linearization around zero (steady state), the second order linear equations of motion are derived:

$$\mathbf{M}\{\ddot{q}\} + \mathbf{C}\{\dot{q}\} + \mathbf{K}\{q\} = \{F\} \tag{4}$$

where $\mathbf{M}$ is the mass matrix, $\mathbf{C}$ is the damping matrix, $\mathbf{K}$ is the stiffness matrix, $\{F\}$ is the force vector and

$$\{q\} = [\theta_{zP0},\, \theta_{zP1},\, u_{yP0},\, u_{yP1},\, \theta_{xP0},\, \theta_{xP1},\, \theta_{xR1},\, \theta_{xR2},\, \theta_{xR3},\, \theta_{xR4}]^T \tag{5}$$

By using a Rayleigh type damping model and assuming that the damping is only stiffness proportional, $\mathbf{C}$ is given as

$$\mathbf{C} = \beta\,\mathbf{K} \tag{6}$$

where β is the stiffness proportional Rayleigh parameter. In the model $\beta = 0.12$ to take account for structural and aerodynamic damping.

Rewriting (3) in first-order form, yields the state-space representation of the system:

$$\begin{aligned} \{\dot{x}\} &= \mathbf{A}\{x\} + \mathbf{B}\{u\}, \\ \{y\} &= \mathbf{C_y}\{x\} \end{aligned} \tag{7}$$

where $\{x\} = [\{q\}, \{\dot{q}\}]^T$ is the state vector, $\{u\} = [F_{t_{R1}}, F_{t_{R2}}, F_{t_{R3}}, F_{t_{R4}}]^T$ is the output vector containing the rotor trust forces. $\mathbf{A}$ is the state matrix given by

$$\mathbf{A} = \begin{bmatrix} \mathbf{0} & \mathbf{I} \\ -\mathbf{M}^{-1}\mathbf{K} & -\mathbf{M}^{-1}\mathbf{C} \end{bmatrix} \tag{8}$$

where $\mathbf{I}$ is the identity matrix, $\mathbf{B}$ is the input matrix and $\mathbf{C_y}$ is the output matrix.

III. SIMULINK SIMULATION MODEL

As a part of the development of the SimWindFarm toolbox and the Aeolus FP7 project a Simulink model for the NREL 5-MW reference turbine was developed [17]. Four of these NREL 5-MW simulink models are connected to connected to the MRT simulink model as seen in Fig. 4.

Each NREL simulink model contains the aerodynamically model as seen in (9) with C_p and C_t look-up tables

$$\begin{aligned} P &= \frac{1}{2}\rho v^3 \pi r^2 C_P \\ T &= \frac{1}{2}\rho v^2 \pi r^2 C_T \end{aligned} \tag{9}$$

where P is the power, T is the thrust, ρ is the air density, v is the wind speed, r is the rotor radius, C_P is the power coefficient and C_T is the thrust coefficient.

Furthermore, they each have a mass-spring-damper model for representing the drive train, a generator efficiency model, a 1-DOF fore-aft tower displacement model, pitch servo and rotor control. The controller is a PI controller which regulates speed using pitch and power. For more information about the models, see [17]. The original SWF tower model is replaced with a 10-DOF model representing the important dynamics of the MR support structure. This model takes thrust forces from the 4 SRTs as inputs and feedback the positions and velocities of the tower top sections, $P0$ and $P1$.

The Simulink setup is illustrated in the simplified diagram seen in Fig. 4. Running the simulation is just a matter of connecting the input to the outputs.

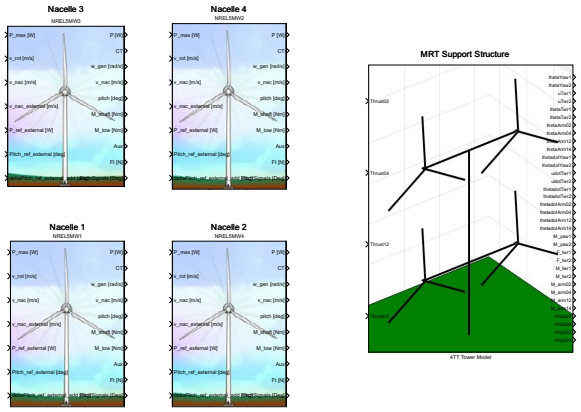

Fig. 4: Simplified Simulink model with four SimWindFarm rotors and nacelles and an MRT support structure model.

The 5-MW NREL Simulink blocks have been modified to support a switch to decouple the original production controller and use an external controller instead.

In order to reuse the wind field generator from [17], four SRTs are equally spaced on a row with 10 % of the rotor diameter, D, as seen in Fig. 5. The wind field has a length of $L_x = 1e3$ m and a width of $L_y = 1.5e3$ m with a grid resolution of 15 m. In order to accommodate for the shear effect on the top rotors, a wind shear contribution is added. The wind profile power law is used to calculate this contribution with an power exponent of $\alpha = 0.15$ representing a smooth grass-covered landscape [19]. This method has limitations and will not capture aerodynamic interaction between the rotors but the dominating aerodynamics effects are taken into account.

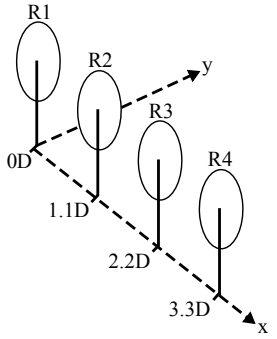

Fig. 5: Wind-field generated for the MRT using "gen_windfield.m" from [17]

In addition an animation feature is available enabling visualization of the simulated time series. Animation of the simulated turbine is a great tool to visualize the different mode shapes as well as the overall behavior of the MRT structure.

The Simulink model including necessary simulated wind fields and documentation is distributed from `https://github.com/kihso/MRTCC`.

IV. CONTROL PROBLEM

The control problem can be structured into five areas: objective, actuators, sensors, models, and operational conditions. The control objective is to have a high annual energy production (AEP), low fatigue loads and a safe operation within specified limits.

The available actuators are equal to those of the SRT i.e. blade pitch angles and generator power (torque). The available sensors are generator speed and nacelle accelerometers. The actual wind speed can be assumed measured or estimated. Furthermore all states of the simulation model (5) are available as sensors. Varying environmental parameters and safety related operating conditions are also important to consider.

By combining choices for each of the five areas, many different control problems of varying complexity can be defined. It is difficult to combine energy production, fatigue loads and safety compliance into a single scalar performance indicator to be optimized.

V. CONTROLLER DESIGN

In this section, an initial controller solution is presented. This gives developers inspiration to design their own baseline MRT controllers. This BLC manipulates each individual rotor pitch reference signal by adding an extra pitch term as seen in Fig. 6. The linear model matrices (7) are assumed known and the whole structural state vector x is assumed measurable.

The input u to the structure are the four SRT thrust forces, $F_{t_{R1}} ... F_{t_{R4}}$. A controller is designed using the classic dynamic equation 10.

$$F_{\mathrm{t}} = M\ddot{y} + D\dot{y} + Ky \tag{10}$$

where y is the tower position and the first and second derivate, and M, D and K are the mass, dampening and stiffness matrix. For more information about the original controller generating F_t see [17]. Adding a delta thrust ΔF_t to dampen structural movements yields 11.

$$F_{\mathrm{t}} + \Delta F_{\mathrm{t}} = M\ddot{y} + D\dot{y} + Ky \tag{11}$$

It is assumed there is a linear relationship between ΔF_t and θ as seen in 12, due to lift being approximated as linear towards angle of attack. This assumption falls apart as θ approaches the stall limits. Furthermore we assume that the arms are relatively stiff in their fore-aft bending.

$$\Delta F_{\mathrm{t}} = \frac{\partial F_t}{\partial \theta}\Delta\theta \tag{12}$$

The control action $\Delta\theta$ is defined in 13 as the linear combination of tower displacement and velocities.

$$\Delta\theta = k_1\,\dot{y} + k_2\,y \tag{13}$$

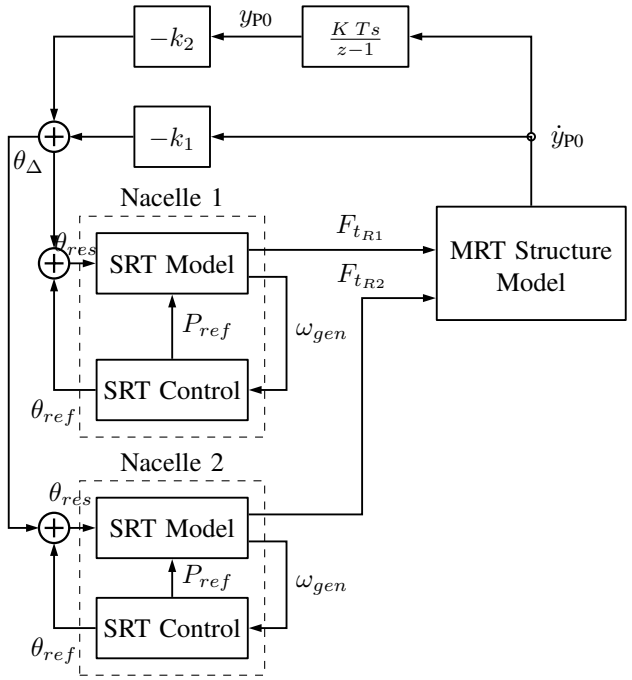

Fig. 6: Control diagram of Baseline Controller (BLC). The lower tower section top-node, $P0$, velocity and integrated velocity (position) are feedback through two gains k_1 and k_2 producing $\Delta\theta$ to manipulate the original pitch reference, θ_{ref} for both lower nacelles 1 and 2. The same control scheme is applied for the two upper nacelles

Combining the equations in 14,15 and 16 and applying the control action for two adjacent rotors, R1 and R2, with individual gains, yields:

$$F_{t_{R1}} + F_{t_{R2}} + \frac{\partial F_{t_{R1}}}{\partial\theta}\Delta\theta + \frac{\partial F_{t_{R2}}}{\partial\theta}\Delta\theta = M\ddot{y} + D\dot{y} + Ky \tag{14}$$

$$F_{t_{R1}} + F_{t_{R2}} + \frac{\partial F_{t_{R1}}}{\partial\theta}(k_{11}\,\dot{y} + k_{21}\,y) + \frac{\partial F_{t_{R2}}}{\partial\theta}(k_{12}\,\dot{y} + k_{22}\,y) = M\ddot{y} + D\dot{y} + Ky \tag{15}$$

$$F_{t_{R1}} + F_{t_{R2}} = M\ddot{y} + \left(D - \frac{\partial F_{t_{R1}}}{\partial\theta}k_{11} - \frac{\partial F_{t_{R2}}}{\partial\theta}k_{12}\right)\dot{y} + \left(K - \frac{\partial F_t}{\partial\theta}k_{21} - \frac{\partial F_t}{\partial\theta}k_{22}\right)y \tag{16}$$

This ultimately gives the option of manipulating the dampening and stiffness of modes by using the resulting pitch signal shown in 17.

$$\theta_{\mathrm{res}} = \theta_{\mathrm{ref}} + \Delta\theta \tag{17}$$

Here θ_{ref} is the original pitch reference signal from the SRT controller, $\Delta\theta$ is the additional pitch signal added from the BLC and θ_{res} is the resulting pitch signal. k_1 and k_2 are the feedback gains on tower top velocity and position, respectively as shown in Fig. 6.

In the simulation model a discrete time controller using the standard NREL 5 MW sampling frequency of 80 Hz is used. This is assumed to be so fast that the above control design method for the continuous system will perform almost the same in the discrete time system.

VI. Test of the Controller

For simplicity, the BMC comparison is done with normal turbulence conditions. The following plots are from 12 m/s wind speeds.

The controller is tuned by finding an input weight k_1 and k_2 that comply with the controller requirements in Tab. III. We start at an arbitrarily high working value $k_1 = 5$ and decrease the value until the evaluation parameters are within an acceptable range. Afterwards the same tuning strategy is applied for $k_2 = 5$.

After some quick ad hoc manual tuning the numeric values for the gains resulted in Tab. VI.

TABLE VI: Controller gain table

k_1 **and** k_2 **values for** $P0$ **and** $P1$									
Parameter	**Wind speed**								
	4	**6**	**8**	**10**	**12**	**14**	**16**	**18**	**20**
k1 at P0	0.1	0.1	0.1	0.1	0.1	0.1	0.1	0.1	0.1
k2 at P0	3.0	3.0	3.0	3.0	1.0	3.0	3.0	3.0	3.0
k1 at P1	0.1	0.1	0.1	0.1	0.1	0.1	0.1	0.1	0.1
k1 at P1	1.0	1.0	0.5	1.0	3.6	5.0	5.0	1.0	1.0

The chosen value for the velocity feedback gain is $k_1 = 0.1$ for all nine wind speeds on both platform. Using this value almost disabled this feedback as seen in velocity pitch signal contribution in Fig. 8. We discovered that this damping term only showed limited performance increases thus kept small. The position feedback greatly helped stabilizing and reducing the structural movements. Good performance was achieved with a value of $k_1 = 3$ for the lower platform $(P0)$. For the upper platform $(P1)$ this gain was a more challenging and required additional tuning. A value of $k_1 = 1$ for high and low all wind speeds was chosen. Near rated wind speed a higher gain is needed, $k_1 = 3.6, 5, 5$ for 12,14, and 16 m/s respectively, to control the structural velocities. This indicates that near maximum thrust, more active control is required. Overall, there is a clear offset tendency with the position feedback pitching out to an offset as seen from the pitch signal components plot in Fig. 8.

Fig. 7 shows the resulting pitch angles θ_{res} for the upper and lower rotors. In the upper plot the BMC is operating in a very aggressive fashion pitching quickly in and out. This is likely due to the significant increases in tower movements, especially for the upper tower section and rotors. In Fig. 9 the upper nacelle velocities are a factor 10 larger than the lower rotors.

The BMC controller have not been tuned for this new tower structure and is having hard a time controlling the generator speed resulting in poor performance. The generator speed, ω_{gen}, is shown in the bottom plot of Fig. 10 which

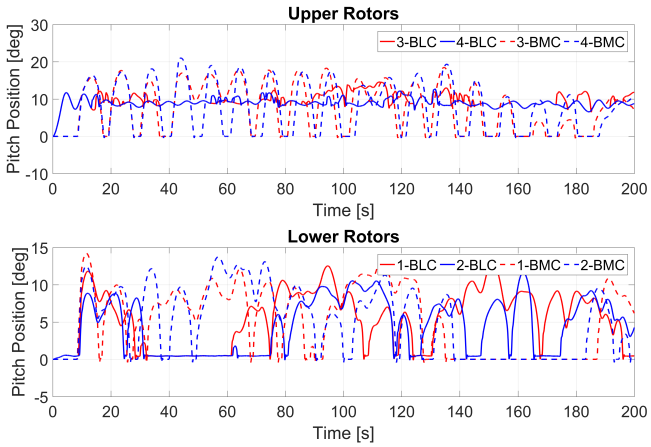

Fig. 7: Resulting pitch signal components θ_{res} for the upper and lower rotors at 12 m/s.

clearly shows the problem. In all aspects the BMC has a much more difficult job of controlling the two upper rotors.

Applying the pitch signals of Fig. 7 reduces the movements of all four nacelles significantly and almost removes excessive oscillations.

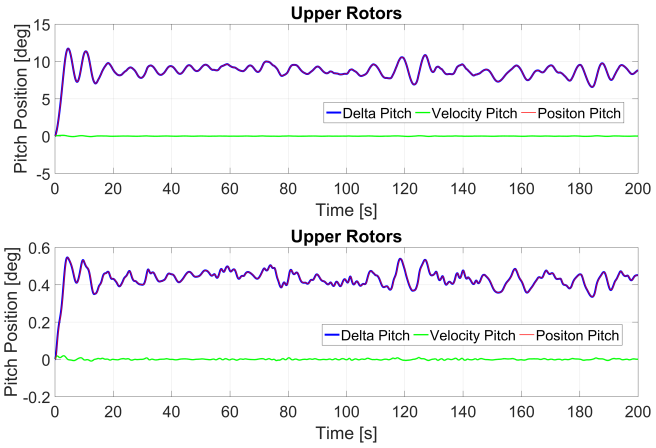

Fig. 8: $\Delta\theta$ pitch signal components for position and velocity feedback for upper and lower nacelles.

The power is also affected by the large variations in generator speeds for the BMC. When the speed is ramping downward the power also drops. The BLC maintains the pitch angles much more static at a quite conservative angle around 9 degrees. This sometimes results in power drops but keeps the tower and nacelle velocities low.

VII. Controller Performance

In order to evaluate the performance of the BLC all indicators from Tab. III are calculated and compared to the BMC. A number below 1 is a numeric reduction in indicator value.

For the first 3 wind speeds the performance of the BLC is almost identical to the BMC. When the wind speed reaches rated wind speed, the influence of the BLC becomes clear. Significant reduction in the tower root moments and also in

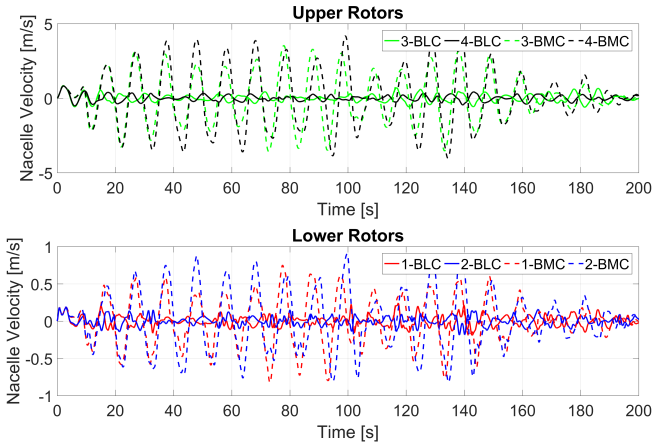

Fig. 9: Upper and lower nacelle velocities for each rotor at 12 m/s.

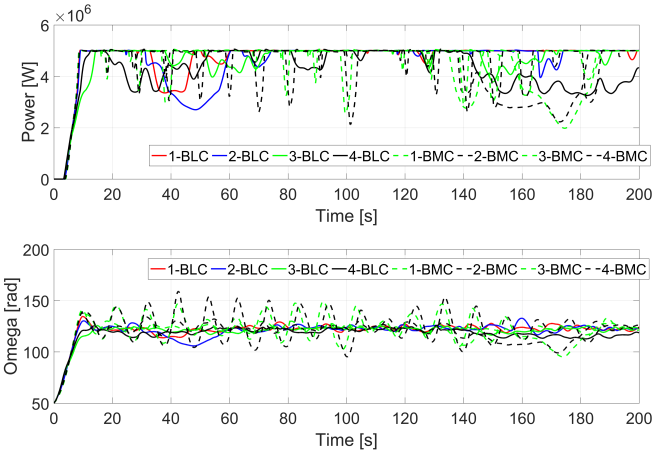

Fig. 10: Power and generator speed plotted for all four nacelles.

the top yaw moment. This is achieved by stiffening the tower with the position feedback. Also for the top arm torsions, large loads reductions are observed. Overall there is superior load reduction on the upper platform compared to the lower.

The loads reductions are obtained but small losses in power are also seen Tab. VIII. A small gain in power production for rotor 2 and 4 is seen at 4 m/s and also for the upper rotors at 16 m/s. This is a bit odd but further investigations and tuning could provide additional power gains.

TABLE IX: Pitch distance traveled comparison for the 4-RT BLC

Pitch Distance Traveled (PDT) [Degrees]										
Parameter	**Wind speed**									**Total Sum (Ratio)**
	4	**6**	**8**	**10**	**12**	**14**	**16**	**18**	**20**	
PDT1	8	10	11	59	194	204	215	162	117	979 (0.91)
PDT2	8	10	11	92	189	234	207	140	135	1026 (0.88)
PDT3	14	17	12	168	230	193	291	124	163	1212 (0.43)
PDT4	14	17	12	134	167	186	294	134	126	1083 (0.25)

Also for the PTD there is a clear benefit for the upper rotors with a reduction of 60-70 % in pitch activity. This is likely due to the more stationary pitching behavior of the BLC.

TABLE VII: Damage equivalent loads ratio comparison between the BLC and BMC.

Damage Equivalent Loads [Nm]										
Parameter	**Wind speed**									**Total**
	4	**6**	**8**	**10**	**12**	**14**	**16**	**18**	**20**	
Twr root Mxy	1.00	0.94	0.94	0.69	0.45	0.48	0.40	0.28	0.33	0.42
Yaw Mz 1	1.00	0.98	0.94	0.88	0.95	0.86	0.90	0.50	0.50	0.76
Yaw Mz 2	0.99	0.95	0.92	0.79	0.54	0.46	0.68	0.15	0.21	0.40
Arm Mx 1	1.01	0.98	0.98	0.86	1.04	0.96	1.05	0.69	0.76	0.90
Arm Mx 2	1.01	0.99	0.95	0.93	1.01	0.97	0.94	0.63	0.67	0.86
Arm Mx 3	0.99	0.99	0.97	0.71	0.46	0.50	0.41	0.39	0.73	0.52
Arm Mx 4	0.99	0.95	1.05	0.70	0.41	0.40	0.40	0.20	0.23	0.36

TABLE VIII: Power comparison for the 4-RT BLC

Mean Power Production [W]										
Parameter	**Wind speed**									**Total**
	4	**6**	**8**	**10**	**12**	**14**	**16**	**18**	**20**	
Power 1	0.99	1.01	0.98	0.94	0.97	0.98	0.98	0.97	0.97	0.97
Power 2	1.02	1.00	0.95	0.94	0.97	0.99	0.98	0.97	0.97	0.97
Power 3	0.99	0.98	0.94	0.96	0.97	0.87	1.03	1.00	0.98	0.97
Power 4	1.03	0.98	0.97	0.95	0.91	0.89	1.03	1.00	1.00	0.97

To do a proper assessment of the BLCs viability to control the MRT, all weather conditions should be evaluated. The velocity feedback term is for this controller almost disabled but could potentially provide more dampening to the structure and improve the overall performance for the controller.

VIII. CONCLUSION

This paper presents the problem of controlling a multi-rotor wind turbine. A model for a 4-RT system is developed. The model is then implemented into a Simulink environment and this Simulink model is offered for all researchers to develop and benchmark advanced control solutions. As an example, a control solution is developed. The solution reduces the structural movements and the damage equivalent loads at the cost of 3 % power loss. Significant improvements in pitch activity are also obtained. The authors hope that this challenge and the availability of the simulation model can encourage researchers to implement and test their control algorithms and to present the results for benchmarking against colleagues around the world.

REFERENCES

[1] "Wind Energy - The Facts." http://www.wind-energy-the-facts.org/growth-of-wind-turbine-size.html. Accessed: 2018-01-11.

[2] G. Sieros, P. Chaviaropoulos, J. D. Soerensen, B. Bulder, and P. Jamieson, "Upscaling wind turbines," *Wind Energy*, 2012.

[3] P. Verma, "Multi rotor wind turbine design and cost scaling," Master's thesis, University of Massachusetts Amherst, 2013.

[4] P. Jamieson and M. Branney, "Multi rotors; a solution to 20 mw and beyond?," *Energy Procedia*, vol. 24, pp. 52–59, 2012. Elsevier Ltd.
[5] H. A. Habib, S. Ibrahim, and I. A. Rafukka, "Multi- rotor wind turbine," *International Journal of Engineering Science and Computing (IJESC)*, vol. 6, no. 5, pp. 4989–4994, 2016.
[6] P. Jamieson and M. Branney, "Structural considerations of a 20mw multi-rotor wind energy system," in *Journal of Physics: Conference Series*, 2014.
[7] E. Bossanyi, "Individual blade pitch control for load reduction," *Wind energy*, vol. 6, no. 2, pp. 119–128, 2003.
[8] S. C. Thomsen, H. Niemann, and N. K. Poulsen, "Stochastic wind turbine control in multiblade coordinates," in *American Control Conference (ACC), 2010*, pp. 2772–2777, IEEE, 2010.
[9] G. Bir, "Multi-blade coordinate transformation and its application to wind turbine analysis," in *46th AIAA aerospace sciences meeting and exhibit*, p. 1300, 2008.
[10] C. Johnson, "Adaptive controller design using disturbance-accommodation techniques," *International Journal of Control*, vol. 42, no. 1, pp. 193–210, 1985.
[11] K. Stol and M. Balas, "Full-state feedback control of a variable-speed wind turbine: a comparison of periodic and constant gains," *Journal of solar energy engineering*, vol. 123, no. 4, pp. 319–326, 2001.
[12] D. Söffker, T.-J. Yu, and P. C. Müller, "State estimation of dynamical systems with nonlinearities by using proportional-integral observer," *International Journal of Systems Science*, vol. 26, no. 9, pp. 1571–1582, 1995.
[13] A. Fakharzadeh, F. Jamshidi, and L. Talebnezhad, "New approach for optimizing energy by adjusting the trade-off coefficient in wind turbines," *Energy, Sustainability and Society*, vol. 3, no. 1, p. 19, 2013.
[14] T. Pan and Z. Ma, "Wind turbine individual pitch control for load reduction based on fuzzy controller design," *Proceedings of the Institution of Mechanical Engineers, Part I: Journal of Systems and Control Engineering*, vol. 227, no. 3, pp. 320–328, 2013.
[15] T. G. Hovgaard, S. Boyd, and J. B. Jørgensen, "Model predictive control for wind power gradients," *Wind Energy*, vol. 18, no. 6, pp. 991–1006, 2015.
[16] J. Jonkman, S. Butterfield, W. Musial, and G. Scott, "Definition of a 5-mw reference wind turbine for offshore system development," Tech. Rep. NREL/TP-500-38060, National Renewable Energy Laboratory, February 2009.
[17] "SimWindFarm." `http://www.ict-aeolus.eu/SimWindFarm/index.html`. Accessed: 2018-01-11.
[18] D. Standards, *Wind turbines âĂŞ Part 1: Design requirements*. DS, 2006, edition 2.
[19] "The Engineering Toolbox." `https://www.engineeringtoolbox.com/wind-shear-d_1215.html`. Accessed: 2018-05-16.
[20] G. F. Franklin, J. D. Powell, and A. Emami-Naeini, *Feedback Control of Dynamic Systems*. Prentice Hall, fourth ed., 2002.
[21] J. Jonkman, S. Butterfield, W. Musial, and G. Scott, "Definition of a 5-mw reference wind turbine for offshore system development," Tech. Rep. NREL/TP-500-38060, National Renewable Energy Laboratory, 1617 Cole Boulevard, Golden, Colorado, USA, 2009.